Journal of Alloys and Compounds 509 (2011) 6175–6183

Contents lists available at ScienceDirect

Journal of Alloys and Compounds

journal homepage: www.elsevier.com/locate/jallcom

Review

Sintering of $BaZrO_3$ and $SrZrO_3$ perovskites: Role of substitutions by yttrium or ytterbium

B. Bendjeriou-Sedjerari[a], J. Loricourt[b,c], D. Goeuriot[a,*], P. Goeuriot[a]

[a] Mechanics and Material Processing, UMR CNRS 5146, Ecole Nationale Superieure des Mines de Saint-Etienne,158 cours Fauriel, 42023 Saint-Etienne cedex 2, France
[b] Societe des Ceramiques Techniques, BP 9,65460 Bazet, France
[c] AREVA NP-NTCI-F, Université Montpellier II (CC 13000), Place Eugene Bataillon, 34095 Montpellier cedex 5, France

ARTICLE INFO

Article history:
Received 16 November 2010
Received in revised form 16 February 2011
Accepted 17 February 2011
Available online 23 February 2011

Keywords:
Perovskite
Sintering
Lanthanide
Tolerance factor
Octahedral factor

ABSTRACT

The modification of perovskite sintering oxides $A^{II}B^{IV}O_3$ was studied. The alkaline earth metal plays a role in the densification of perovskite. The effect of the substitution of Zr^{4+} by a lanthanide Yb^{3+} in barium zirconate (BZYb) increases its density and impedes BaO evaporation independently of the thermal cycle. A substitution of Zr^{4+} by Y^{3+} increases the density of barium zirconate (BZ) only after 4 h at 1650 °C. In all cases, the substitutions of Zr^{4+} by Y^{3+}or $Yb^{2+\text{ or }3+}$ in the zirconate inhibit grain growth. The substitution in B site by a Ln^{3+} leads to the creation of vacancies ($A^{II}B^{IV}_{(1-x)}Ln^{III}_x O_{3-x/2}$). To determine the vacancies' role, three different controlled atmospheres were tested. Argon, dry air, and oxygen were used to study the impact on the linear shrinkage of barium zirconate when some Zr^{4+} are replaced by yttrium or ytterbium (BZY, BZYb) or not substituted (BZ). Strontium zirconate (SZ) is not as chemically stable as barium zirconate (BZ) during the thermal cycle when Yb is used as a substitution element. In effect, the presence of the secondary phase $Zr_3Yb_4O_{12}$ associated with the release of oxygen proves the bivalence of ytterbium (Yb^{2+} or Yb^{3+}). Therefore, ytterbium can be substituted in either A or/and B sites. The study of reactive sintering between lanthanum strontium zirconate (SZYb) and Yb_2O_3 shows that a slight excess of Yb_2O_3 around SZYb grains stabilizes the chemical composition of SZYb. Perovskite symmetry and stability were determined by two factors, i.e., tolerance (t) and octahedral factors (r_B/r_O). It was demonstrated that the distortion of the perovskite unit cell increases the density of pellets.

Contents

* Corresponding author. Tel.: +33(0)4 77 42 01 92; fax: +33(0)4 77 42 02 49.
E-mail address: dgoeurio@emse.fr (D. Goeuriot).

0925-8388/$ – see front matter © 2011 Elsevier B.V. All rights reserved.
doi:10.1016/j.jallcom.2011.02.088

Table 1
Nomenclature of synthesized zirconate (formulation was determined by ICP-AES).

Composition synthesized	Nomenclature
$BaZrO_3$	BZ
$BaZr_{0.97}Y_{0.03}O_{2.985}$	BZY
$BaZr_{0.97}Yb_{0.03}O_{2.985}$	BZYb
$SrZrO_3$	SZ
$SrZr_{0.93}Yb_{0.07}O_{2.965}$	SZYb

1. Introduction

$BaZrO_3$ and $SrZrO_3$perovskite-type oxides are mainly studied because of their application in high temperature electrochemical systems, such as Solid Oxide Fuel Cell (SOFC) and oxygen sensors. Zirconate phases present many properties: adequate ionic conduction, high melting point, low thermal expansion coefficient, and a high dielectric constant [1–10]. It is possible to create defects in the perovskite structure by proper doping in order to either create oxygen deficient compositions or solids solutions of the parent perovskite with another perovskite [1,7]. Many perovskite-type phases show protonic conduction at high temperatures when doped with acceptor ions. For example, when trivalent cations such as Ln^{3+} substitute tetravalent ions such as Zr^{4+}, oxygen ion vacancies are introduced into the crystal to keep the charge balance ($A^{II}B^{IV}_{(1-x)}Ln^{III}_xO_{3-x/2}$). These oxides have a large potential for use in fuel cell, steam electrolysis, and hydrogen gas sensors [4] and are crucial for future prospect of renewable energy. The sintering of perovskite phases is performed from synthesized powder (from precursors) or by solid state reaction densification, with or without sintering aids [11,12].

The aim of this study is to correlate the composition with sintering behaviors of different perovskite systems. For this purpose, the use of different cations in A site, and doping elements in B site to create oxygen vacancies will be investigated, in relation with the densification of the corresponding materials. It is believed that, due to their different sizes, the ions in substitution could change the diffusion mechanisms during sintering in the distorted cell; the created vacancies could also have a role in the densification process. Thus, after presenting the results dealing with the densification, a discussion concerning the role of oxygen vacancies and the distortion of the unit cell of perovskite on the densification proposed.

Barium zirconate and strontium zirconate are used as basis for this sintering study. Thus, the effect of alkaline earth metal (Ba/Sr) on the samples density will be compared. The role of the rate of oxygen vacancies introduced by substitution of Zr^{4+} by yttrium or ytterbium (Yb^{2+}, Yb^{3+}) and in some cases oxide additives (Y_2O_3, Yb_2O_3) on the final material's density and microstructure will also be described. Sintering under different atmospheres (oxygen, dry air, argon, hydrogenated argon) of substituted $BaZrO_3$ by Y or Yb will complete the anionic vacancies' influence on density.

The final discussion will concern the relationship between sinterability and unit cell distortion (described by the tolerance and octahedral factors) obtained by the choice of alkaline-earth and doping (Y and Yb) elements.

2. Experimental details

2.1. Processing

A coprecipitation technique was used in the synthesis of perovskite powder ($AZrO_3$). This technique was 98% efficient. $A(NO_3)_2$, $Zr(NO_3)_4$ were the starting materials and $D(NO_3)_3$ was in some cases added in stoichiometric quantity to introduce anionic vacancies in the perovskite. The reactants in oxalic acid result in an intermediary product that was calcined to form perovskite white agglomerated powder (grain size around 300 nm). Table 1 reports the characteristics of the perovskite synthesized and the nomenclature chosen.

The agglomerates of powder were dispersed by mechanical agitation and ultrasound in anhydrous ethyl alcohol (50 wt.% of dry matter) containing phosphoric ester (dispersant) to obtain a slurry. The slurry was then milled with stabilized CeO_2 zirconia milling balls (Φ = 1.4 mm) and dried under an extractor hood. The perovskite powder was consolidated by uniaxial pressing pellets (8 mm diameter × 2 mm length) under 300 MPa (INSTRON press). The decomposition temperature of organic phases and the temperature at which perovskite forms made it possible to build the thermal cycle as a function of the atmosphere [9]. In the present study, all samples were calcined under an oxidizing atmosphere at 400 °C to eliminate organic phases before their sintering in a dilatometer.

2.2. Characterization

A vertical dilatometer was employed to measure the axial shrinkage of pellets during the thermal cycle. Perovskite pellets were placed between two sintered zirconia wedges to avoid perovskite pellets sticking to the alumina transducer. The displacement transducer was positioned on the surface of the zirconia wedge with a charge of 10 g. Linear shrinkage of the perovskite pellet was studied under controlled atmosphere (dried air, argon, hydrogenated argon) from 20 °C to 1650 °C (5 °C/min) with or without a 4 h dwell at 1650 °C. The thermal cycle under air atmosphere had an additional isotherm of 3 h at 900 °C.

The densification rate was measured by Archimed's method. The theoretical density ρ_{th} was that of the perovskite of the minor phases. The gain of density was defined as the difference between final and green densities.

The microstructures fractures of samples were investigated on a FEG-SEM (JEOL JSM-6500F.

The crystal structure of the sample was analyzed by X-ray diffraction at room temperature using Cu Kα radiation. Pattern Matching method from the software Topaz-2P was employed to refine the lattice parameters evolution of $SrZrO_3$.

The ytterbium valency was detected by XPS analysis. The XPS measurements were conducted by THERMO VG, THETAPROBE with Al Kα radiations (pass energy EP = 50 eV, ΔE = 0.55 eV for Ag $3d_{5/2}$). Instrumental resolution is around 0.1 eV. The analysis was performed under ultrahigh vacuum (6×10^{-10} mbar). Sample surfaces were cleaned in situ by Ar^+ ion bombardment at 1 keV.

3. Results and discussion

3.1. Effect of alkaline earth metals on the sinterability of perovskite type $AZrO_3$

Two alkaline earth types, barium or strontium were used in A^{2+} site. Dilatometric and hydrostatic density measurements showed that the strontium zirconate was denser than barium zirconate (Fig. 1). The influence of the nature of alkaline earth was observed during heating. Effectively, the linear shrinkage rate of barium zirconate formed two peaks. The first one around 1060 °C and the second one at 1540 °C. The linear shrinkage rate of strontium zirconate only has one peak at 1645 °C.

After soaking at 1650 °C, the difference of densification gain between these two zirconates was about 22% D_{th} in favour of strontium zirconate. The microstructure of strontium zirconate (82.2% D_{th}^{final}) presents a grain size close to that of barium zirconate (67.4% D_{th}^{final}) in spite of this densification mismatch (Fig. 2). This proves that grain coarsening occurs faster for the BZ during densification. The 4 h dwell at 1650 °C promotes a coarser grain size in both cases. Zirconate strontium with (96.7% D_{th}^{final}) had an heterogeneous grain size (1–10 μm) with intragranular rupture in the largest grains. Microstructure of barium zirconate (76.2% D_{th}^{final}) presents relatively homogeneous grain size. It suggests that the BZ grains may grow to change the surrounding environment, enhancing the densification process, while it is not the case for the SZ samples.

3.2. Substitution role of zirconium (in site B) by a lanthanide (Y or Yb) in perovskite type $AZrO_3$sintering (with A = Ba or Sr) in air

3.2.1. Case of $BaZrO_3$ substituted by yttrium (BZY) or ytterbium (BZYb)

No secondary phases were observed by XRD on the BZY and BZYb samples sintered at 1650 °C even after 4 h dwell. Whereas, BZ formed a zirconia cubic phase as a secondary phase. BaO was

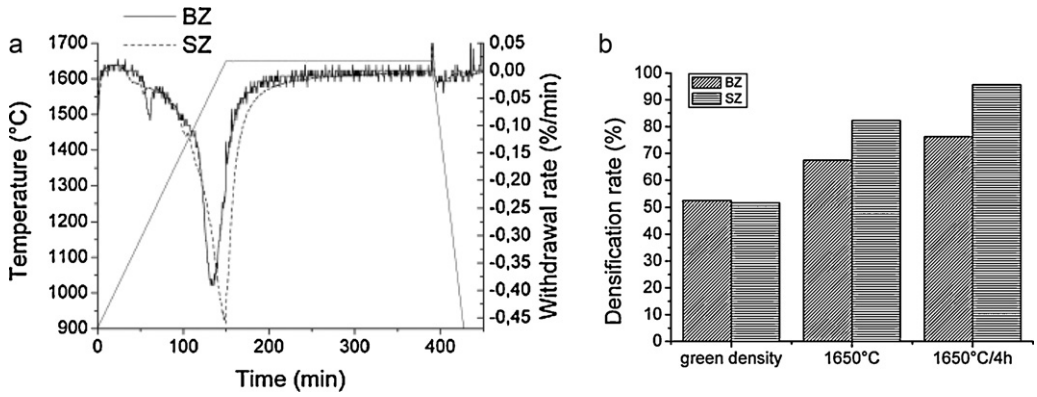

Fig. 1. (a) Alkaline earth elements influence on the zirconate withdrawal rate during a thermal cycle (4 h at 1650 °C) under dried air. (b) Alkaline earth elements influence on the zirconate densification (±0.2%) during a thermal cycle (4 h at 1650 °C) under dried.

not detected by XRD, meaning one part probably volatilized, and the other part is amorphous (as a result it was not possible to take BaO into account for the theoretical densities calculations of the sintered samples). This phenomenon shows that the substitution of a part of zirconium in the structure leads to the stabilization of the perovskite. This substitution is associated with an expansion of the unit cell in both Y and Yb cases (Table 2).

Fig. 3 shows the densification rate of substituted (Y or Yb) and standard barium zirconate after sintering at 1650 °C with or without a 4 h dwell. Ytterbium (Yb) always had a favourable effect on the densification of BZ. Yttrium (Y) was disadvantageous during the rise of temperature. However, it had a positive effect on densification during the rest of the cycle although not as much as Yb. The presence of Y or Yb in the perovskite BZ during sintering reduces the grain size compared with the un-doped BZ one (Fig. 4).

3.2.2. *Case of $SrZrO_3$ substituted by ytterbium (SZYb)*

Just like BZ, $SrZrO_3$ is not stable: zirconia appears as a secondary phase; SZ is stabilized (less than in the case of BZ) by the partial substitution of zirconium by ytterbium. A small percentage of zirconia containing ytterbium is observed. The sintering study of SZ and SZYb shows that Yb did not modify the densification rate of SZ (Fig. 5). However, the gain of densification is highest

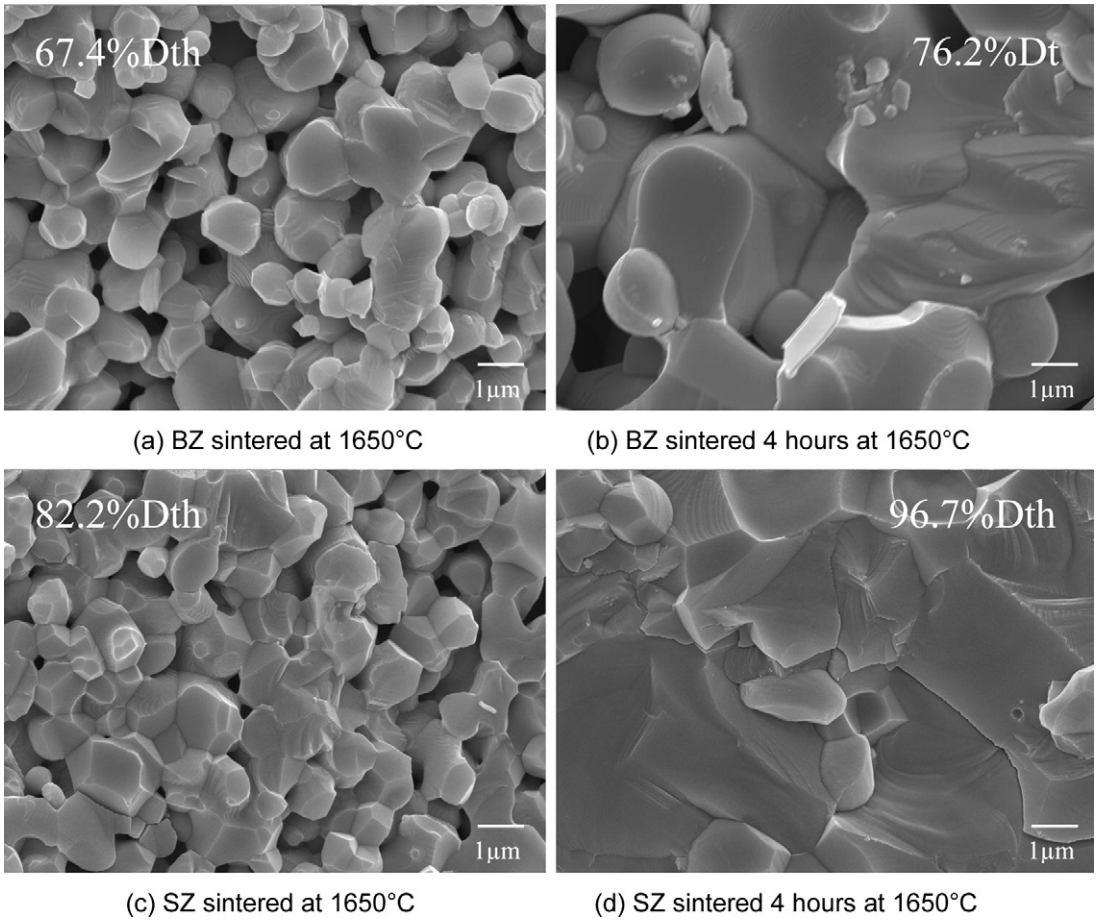

Fig. 2. BZ and SZ microstructure after sintering to 1650 °C (left) and after 4 h 1650 °C (right) under dried air.

Table 2
Effect of ytterbium oxide addition on densification rate, unit cell volume of barium zirconate (cubic) and strontium zirconate (orthorhombic) and nature of secondary phases.

		Unit cell volume (3 ± 0.1 Å)	Secondary phases
BZ	Green	–	–
	1650 °C	73.5	Trace ZrO_2
	1650 °C/4 h	73.5	5–10 wt.% ZrO_2
BZ + 0.03Y	Green	–	–
	1650 °C	73.7	2–3 wt.% $Zr_{3.14}Y_{0.86}O_{7.59}$
	1650 °C/4 h	73.7	2–3 wt.% $Zr_{3.14}Y_{0.86}O_{7.59}$
BZ + 0.07Y	Green	–	–
	1650 °C	73.8	2–3 wt.% Y_2O_3, 2–3 wt.% $Zr_{3.14}Y_{0.86}O_{7.59}$
	1650 °C/4 h	73.8	Trace Y_2O_3, 3–5 wt.% $Zr_{3.14}Y_{0.86}O_{7.59}$
BZY	Green	–	–
	1650 °C	74	No secondary phases
	1650 °C/4 h	74	No secondary phases
BZY + 0.04Y	Green	–	–
	1650 °C	74.1	1–2 wt.%Y_2O_3
	1650 °C/4 h	74.1	1–2 wt.%Y_2O_3, trace $Zr_{3.14}Y_{0.86}O_{7.59}$
BZYb	Green	–	–
	1650 °C	73.9	No secondary phases
	1650 °C/4 h	–	No secondary phases
SZ	Green	–	–
	1650 °C	277.8	Trace ZrO_2
	1650 °C/4 h	277.4	5–10 wt.% ZrO_2
SZ + 0.07Yb	Green	–	–
	1650 °C	277	1–2 wt.% $Zr_3Yb_4O_{12}$
	1650 °C/4 h	277	1–2 wt.% $Zr_3Yb_4O_{12}$
SZ + 0.1Yb	Green	–	–
	1650 °C	277	2–3 wt.% $Zr_3Yb_4O_{12}$
	1650 °C/4 h	277	1–2 wt.% $Zr_3Yb_4O_{12}$
SZYb	Green	–	–
	1650 °C	277.4	Trace $Zr_3Yb_4O_{12}$
	1650 °C/4 h	277.0	1–2 wt.% $Zr_3Yb_4O_{12}$
SZYb + 0.03Yb	Green	–	–
	1650 °C	277.4	Trace Yb_2O_3
	1650 °C/4 h	277.4	Trace Yb_2O_3

Table 3
Densification rate and gain of SZ and SZYb after sintering at 1650 °C or 4 h at 1650 °C.

	% D_{th}	1650 °C Densification gain (%)	% D_{th}	1650 °C/4 h Densification gain (%)
SZ	82.2	30.7	96.7	45.2
SZYb	83.5	35.3	98.9	50.7

for doped samples (Table 3). Furthermore, ytterbium refines the SZ microstructure.

3.3. Reaction sintering for studied systems

Lanthanide oxide powder was mixed with the initial powder to increase the rate of cationic substitution of the perovskite structure

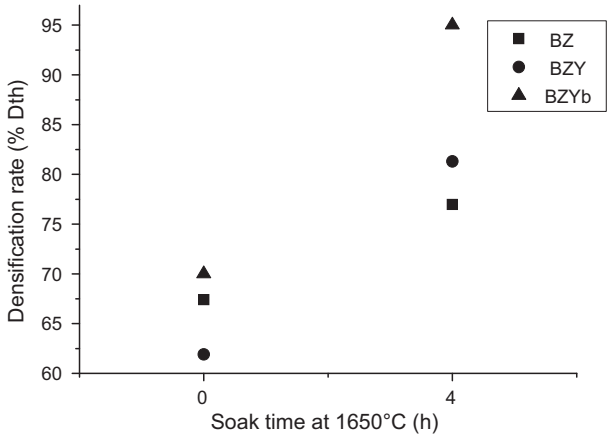

Fig. 3. Densification rate of BZ, BZY, BZYb sintering at 1650 °C or during 4 h at 1650 °C.

(Y_2O_3 and Yb_2O_3 for BZ and for SZ systems, respectively) (Table 4). In every case, the addition of lanthanide oxide decreased the densification rate, as shown in (Fig. 6) and modified the grain size (Fig. 7). Chemical reactions occur during sintering. Yttried zirconia, a secondary phase, is observed for BZ and BZY systems. Ytterbied zirconia is formed for SZ and SZYb systems (Table 2). For previous doped samples, more lanthanide oxides could dissolve in the perovskite structure as demonstrated by the amount of remaining Ln_2O_3 phases (alone or in zirconia) which often decreased during heating (Table 2). In the case of BZ, the dissolution is clear with the evolution of the unit cell volumes. In the case of Yb_2O_3 additions in SZ and SZYb, the unit cell volume changes very slightly. This will be explained in Section 3.5.

Table 4
Mass concentration necessary and nomenclature of mixtape $AZrO_3 + Ln_2O_3$ and $AZr_{1-x}Ln_xO_{3-x/2} + Ln_2O_3$ to obtain desired amount of lanthanide (Y or Yb) around perovskite grains.

Composition	at. %Ln	wt.% Ln_2O_3	Nomenclature
$SrZrO_3$	7	6.54	SZ + 0.07Yb
	10	9.65	SZ + 0.1Yb
$SrZr_{0.93}Yb_{0.07}O_{2.965}$	3	2.62	SZYb + 0.03Yb
$BaZrO_3$	3	1.26	BZ + 0.03Y
	7	3.07	BZ + 0.07Y
$BaZr_{0.97}Y_{0.03}O_{2.985}$	4	1.70	BZY + 0.04Y

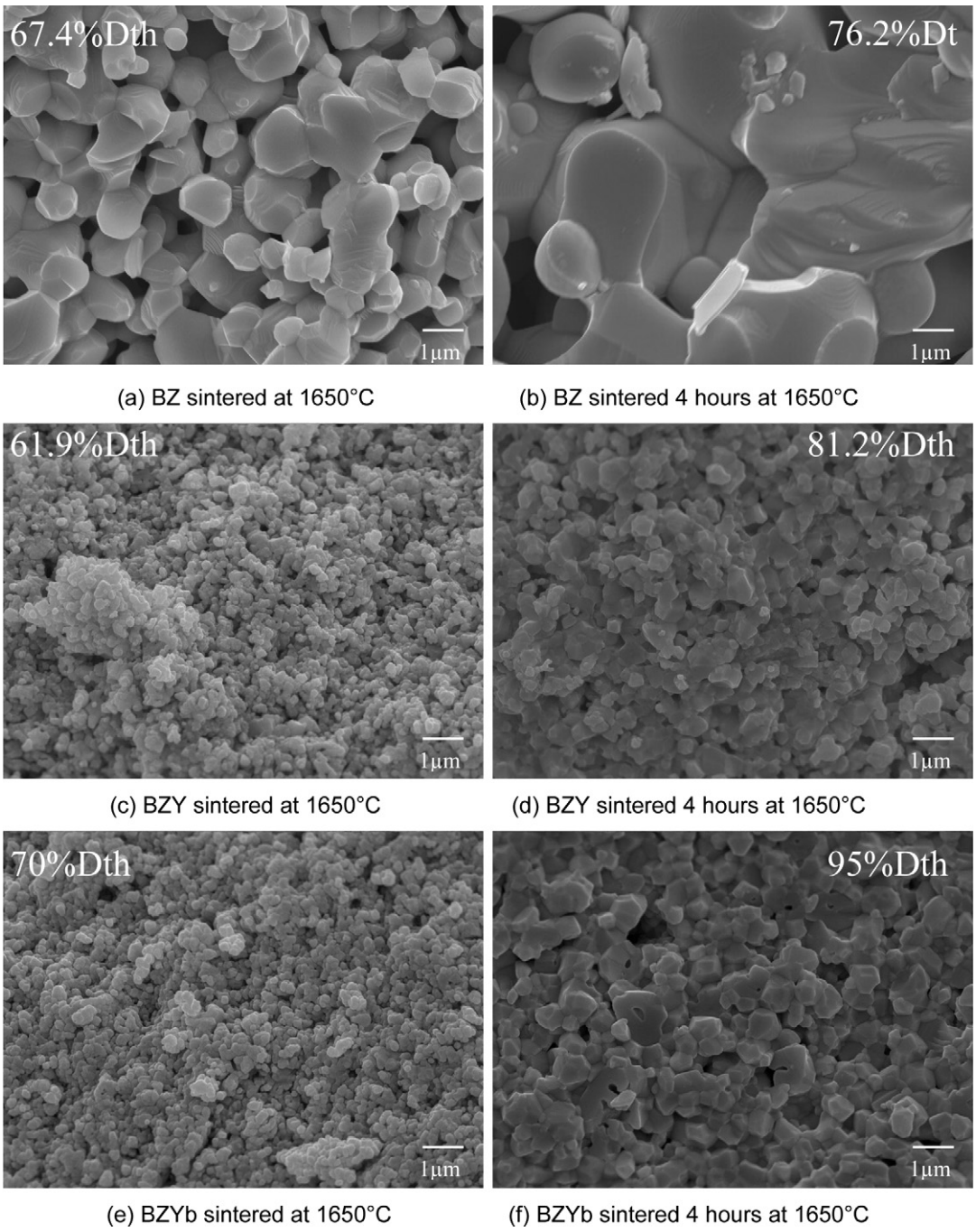

Fig. 4. Effect of zirconium substitution by a lanthanide (Y or Yb) on $BaZrO_3$ microstructure under dried air.

3.4. Role of atmosphere on sintering for BZ-type systems

The influence of atmosphere on sintering was studied for barium zirconate only. Fig. 8 gives the results for gain in density. Both neutral and oxidizing atmospheres have no effect on sintering of BZ. However, a small beneficial effect occurs for the substituted BZ. A reduced atmosphere (Ar–10% H_2) gives the same result as dry air for powder, formulated with binder and plasticizer (BZYb spray dried). The atmosphere had not impact on the grain size.

To conclude, this demonstrates anionic vacancies are not the factor which determines sintering rate.

3.5. Discussion

3.5.1. Reactivity of the studied systems

Our results show that the perovskite powder obtained at low temperature evolves during the heating cycle, in particular in the presence of lanthanide oxide additions. Five theoretical reactions can be used to describe the dissolution of the doping element.

$$ABO_3 + \frac{x}{1-x}D_2O_3 \xrightarrow[1650^\circ C]{\text{sintering}} \frac{1}{1-x}[A_{1-x}D_xB_{1-x}D_xO_3] \quad (1)$$

$$ABO_3 + \frac{x}{2}D_2O_3 \xrightarrow[1650^\circ C]{\text{sintering}} A_{1-x}D_xBO_{3+(x/2)} + xAO \quad (2)$$

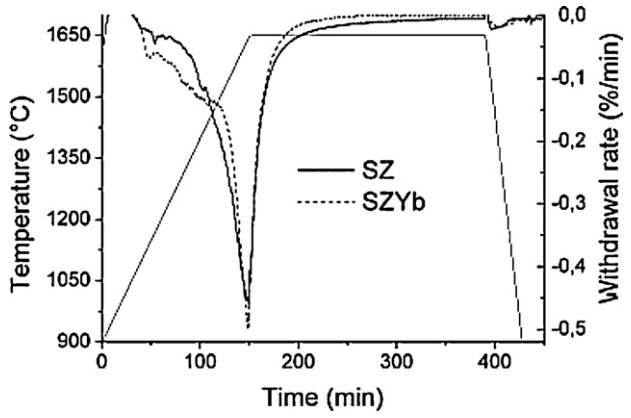

Fig. 5. Effect of substitution by Yb on the withdrawal rate of SZ.

with alkaline oxide and by anionic interstitial formation (note this reaction has a low probability).

$$ABO_3 + \frac{y}{2}D_2O_3 \overset{\text{sintering}}{\underset{1650^\circ C}{\longrightarrow}} AB_{1-y}D^{III}_yO_{3-(y/2)}\square_{(y/2)} + yBO_2 \quad (3)$$

with Zirconia type structure formation (B = Zr).

$$ABO_3 + \frac{x+y}{2}D_2O_3 \overset{\text{sintering}}{\underset{1650^\circ C}{\longrightarrow}} A_{1-x}D_xB_{1-y}D_yO_{3+(x-y/2)} + xAO + yBO_2 \quad (4)$$

if $x > y$ anionic interstitial could exist, which is not realistic.

If D has two valences (II and III), the general case is:

$$ABO_3 + \frac{x+y}{2}D_2O_3 \overset{\text{sintering}}{\underset{1650^\circ C}{\longrightarrow}} A_{1-x}D^{II}_xB_{1-y}D^{III}_yO_{3-(y/2)}\square_{(y/2)} + xAO + yBO_2 + \frac{x}{4}O_2 \quad (5)$$

For Eq. (5) an oxygen release must occur along with the formation of an alkaline oxide and zirconia phases.

According to the residual phases obtained after firing (Table 2), Eq. (3) is the most probable for yttrium oxide substitution in B site.

For Yb substitution, Eq. (5) is the most probable in SZ systems despite the fact SrO is not present on XRD patterns. Two facts confirm this hypothesis: (i) oxygen release has been detected by mass spectrometer during the heat treatment of SZ + Yb_2O_3, (ii) XPS analyses on fractured samples confirm the possibility of obtaining ytterbium with valency 2 (Fig. 9). The unit cell volumes vary only slightly with the substitution. In effect the cell distortion caused by the substitution of Yb^{3+} (larger than Zr^{4+}) is compensated by the substitution of Yb^{2+} (smaller than Sr^{2+}). For SZYb with an excess of Yb_2O_3, the secondary phases SrO and $Zr_3Yb_4O_{12}$, which are probably produced by the evolution of SZYb, could react with the excess to give a pure perovskite.

3.5.2. Sinterabilty of the studied systems

a) Perovskite structure stability criteria

The stability of a cubic structure perovskite was determined by two geometrical factors, tolerance and octahedral [2,13–16].

Goldschmidt [17] used the tolerance factor (t) to study the stability of perovskite as shown in Eq. (6).

$$t = \frac{r_A + r_O}{\sqrt{2}(r_B + r_O)} \quad (6)$$

Where r_A, r_B and r_O are, respectively ionics radii of A, B and O.

This relation is valid only if the sum of valence electrons of A and B is equal to 6 and the number of oxygen is 3. Geometrically, in an ideal perovskite structure, the ratio bond lengths

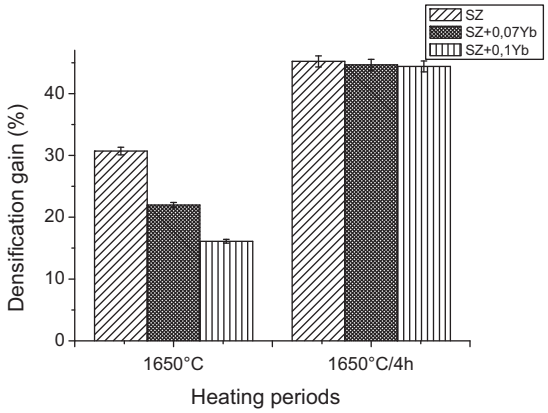

(a) : Effect of Yb_2O_3 grain addition on SZ sintering.

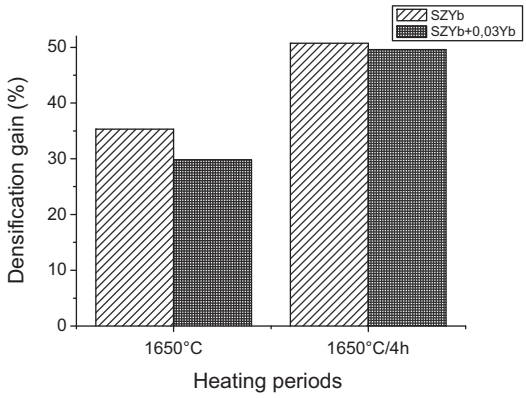

(b) : Effect of Yb_2O_3 grain addition on SZYb sintering.

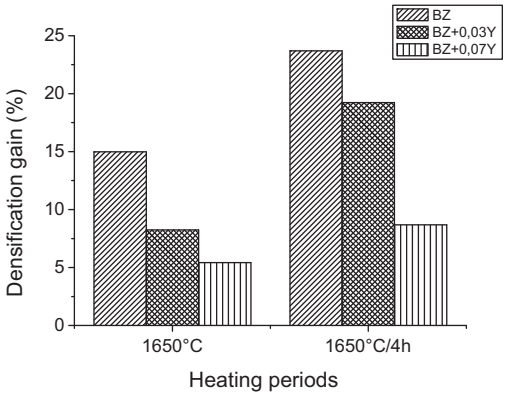

(c) : Effect of Y_2O_3 grain addition on BZ sintering.

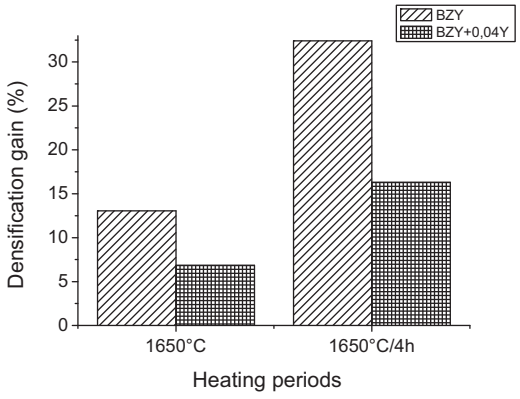

(d) : Effect of Y_2O_3 grain addition on BZY sintering.

Fig. 6. Densification gain (±0.2%) of SZ, SZYb or BZ, BZY sintered in presence of Yb_2O_3 or Y_2O_3, respectively.

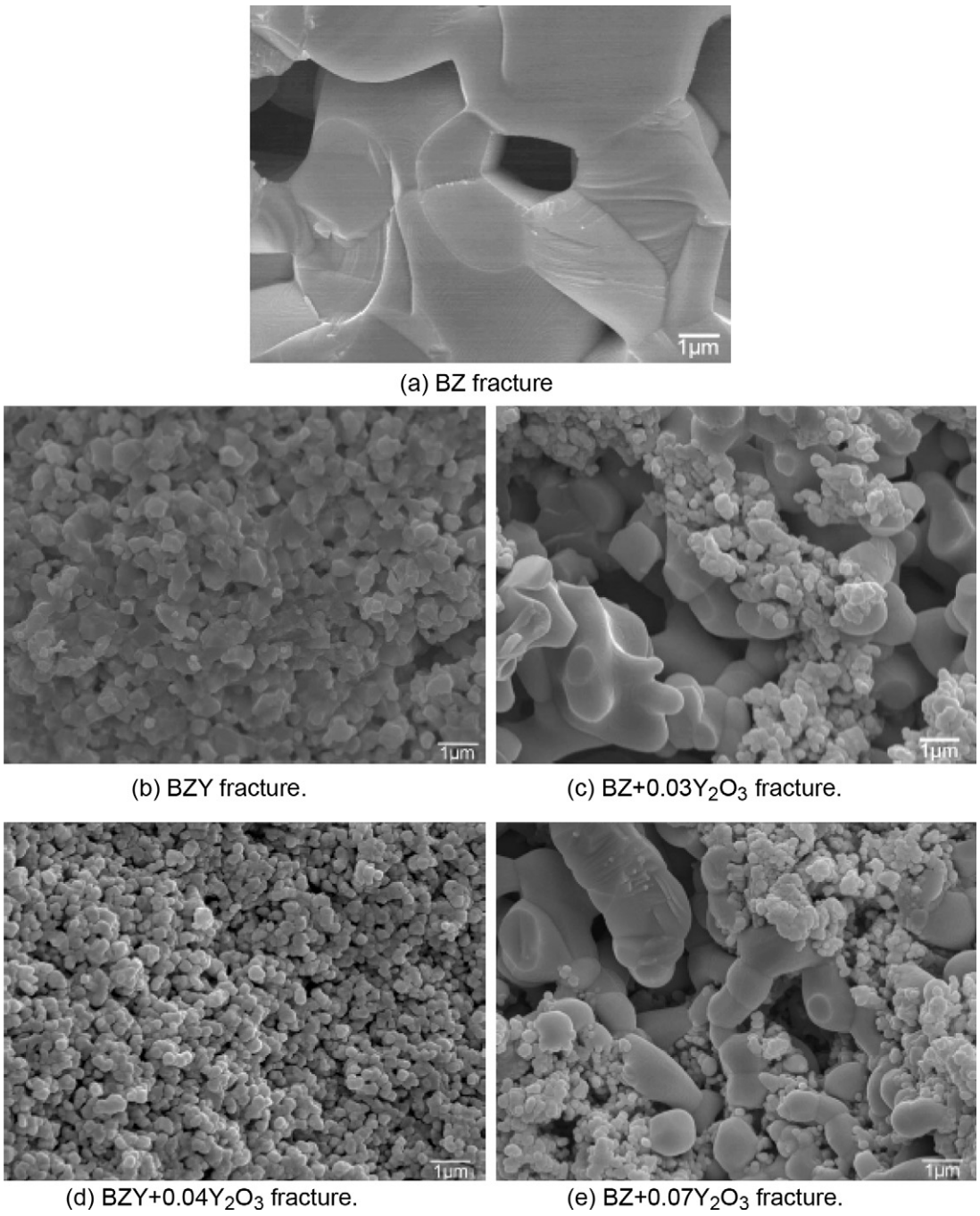

Fig. 7. Effects of Y_2O_3 addition on the microstructure of sintered BZ or BZY at 1650 °C/4 h.

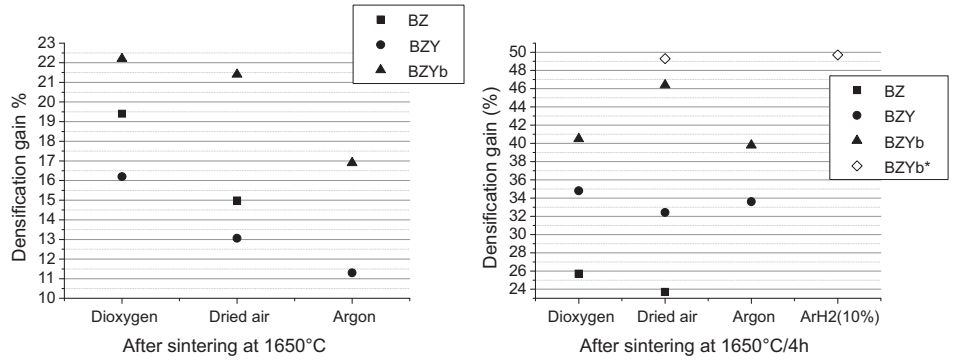

Fig. 8. Densification gain of BZ, BZY, BZYb and BZYb* (spray dried) under diverse controlled atmosphere (oxygen, dried air, argon or hydrogenated argon) before or after 4 h at 1650 °C.

Table 5
Ionics radii of the chemical elements used according to Shannon table.

Ionics radii (Å)	Charge	Coordination										
		II	III	IV	V	VI	VII	VIII	IX	X	XI	XII
Ba	2					1.35	1.38	1.42	1.47	1.52	1.57	1.61
Sr	2					1.18	1.21	1.26	1.31	1.36		1.44
Zr	4			0.59	0.66	0.72	0.78	0.84	0.89			
Y	3					0.9	0.96	1.019	1.08			
Yb	2					1.02	1.08	1.14				1.38[a]
	3					0.868	0.93	0.985	1.04			
Er	3					0.89	0.95	1.004	1.06			
O	−2	1.35	1.36	1.38		1.4	1.42					

[a] Obtened by extrapolation.

A–O and B–O are equal to $\sqrt{2}$. In this case $t = 1$. Goldschmidt found experimentally that t values of most cubic perovskite are in the range of 0.8–0.9. Goldschmidt's tolerance factor t has been widely accepted as a criterion for structural perovskite formation. Moreover, up to now, most known perovskite compounds have t-values in the range of 0.75–1.00. Perovskite structure exhibits octahedral sites (BO_6) which must be interconnected by their oxygen anions (O^{2-}) and form a cubo-octahedral around a cation A^{2+} so that A–O bond length is close to the sum of their ionics radii [9]. The octahedron BO_6 is stable in the range of $0.414 < r_B/r_O < 0.732$ (octahedral factor).

In our case, the calculation of these factors (t and r_B/r_O) considers the ionic radii values for a degree of oxidation and for a coordination number fixed (Table 5). Contrary to some authors [13,18] but similarly to Ullman et al. [16], we have refined tolerance and octahedral factors for substituted perovskite in A or/and B site by cation with different valencies. The pertinence of our choice of ionic radii of cationic elements was accomplished with regard to valency and coordination numbers. Oxygen ionic radius in coordination 2 or 4 is 1.36 Å. Note that these values are issued from Shannon's data [19]. The vacancy radius ($r_{V,o} = 1.36\,V^{1/3}$) was also integrated in the factors' calculation and determined from the free volume of the unit cell, V_f = (unit cell volume – occupied space). Ullman et al. have measured the oxygen deficiencies by solid electrolyte potentiometry and coulometry [20,21]. Thus the tolerance and octahedral factors used in the present study will be:

$$t_{\text{refined}} = \frac{r_A + r_O + x(r_{D^{II}} - r_A) + \frac{y}{6}(r_{V,O} - r_O)}{\sqrt{2}(r_B + r_O + y(r_{D^{III}} - r_B + \frac{r_{V,O} - r_O}{6}))} \quad (7)$$

$$r_{V,O} = 1.36\sqrt[3]{V_{\text{free}}}$$

$$\left(\frac{r_B}{r_O}\right)_{\text{refined}} = \frac{r_B + y\,(r_y - r_B)}{r_O + \frac{y}{2}(r_{V,O} - r_O)} \quad (8)$$

with r_A, $r_{V,A}$, r_O, r_{Vo}, r_B, r_{Ln} being, respectively ionic radii of cation A^{2+}, cationic defect in A site, anion O^{2-}, anionic defect, cation B^{4+} and lanthanide; x and y correspond to the coefficients in Eqs. (3) and (5); V_{free} is the free volume of the unit cell.

b) relationships between the systems sinterability and the corresponding cell distortion

The role of alkaline earth elements and of Zr^{4+} substitution by lanthanide oxides (Y, Yb) in perovskite on the sintering behavior can be linked to the progression of their unit cell formation. A beneficial effect of earth element or substitution on sintering is always associated with distortion of the unit cell (Fig. 10). This is explained by the radii of the chemical species which influences on both tolerance and octahedral factors. It is postulated that the distortion of the perovskite unit cell favours the cationic diffusion meaning the densification process. However, the anionic vacancies have no effect as the results of heat treatments in different atmospheres have demonstrated.

Cations presenting two valences, such as Yb, can be in the position A and/or B in the perovskite structure. Tolerance and octahedral factors refined calculation was performed considering two extreme cases: Yb^{3+} in B site or Yb^{2+} in A site. For strontium zirconate, the first case (Yb^{3+} in B site) leads to a strong decrease in the tolerance and octahedral factors versus the substitution rate. In comparison with the second case (Yb^{2+} in A site), Fig. 11. According to the X-rays and XPS analyses it is assumed that Yb is preferably in B site, and only a small rate in A site. This explains the strong unit cell distortion and the small quantity of obtained secondary phases. In this case, the unit cell distortion also has a beneficial effect on the perovskite densification, as shown in Fig. 10.

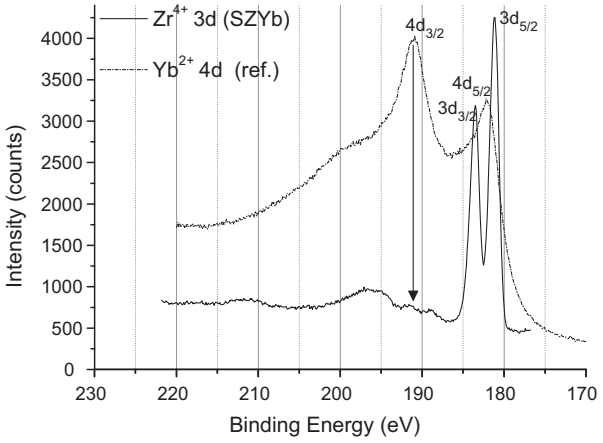

Fig. 9. XPS spectra at the rupture surface of SZYb sintered at 1650 °C.

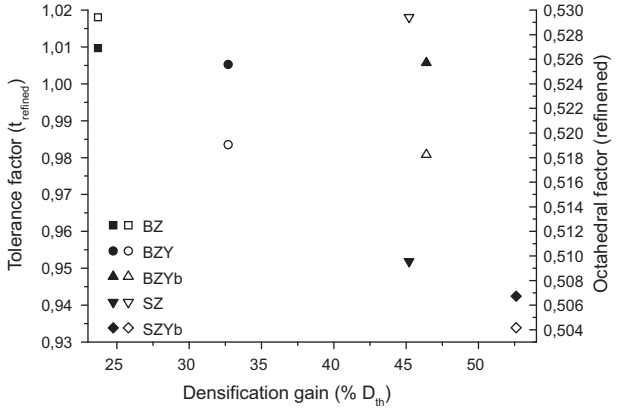

Fig. 10. Influence of the perovskite symetry on pellet densification. Tolerance factor was represented by plain symbol and octahedral factor by empty symbol.

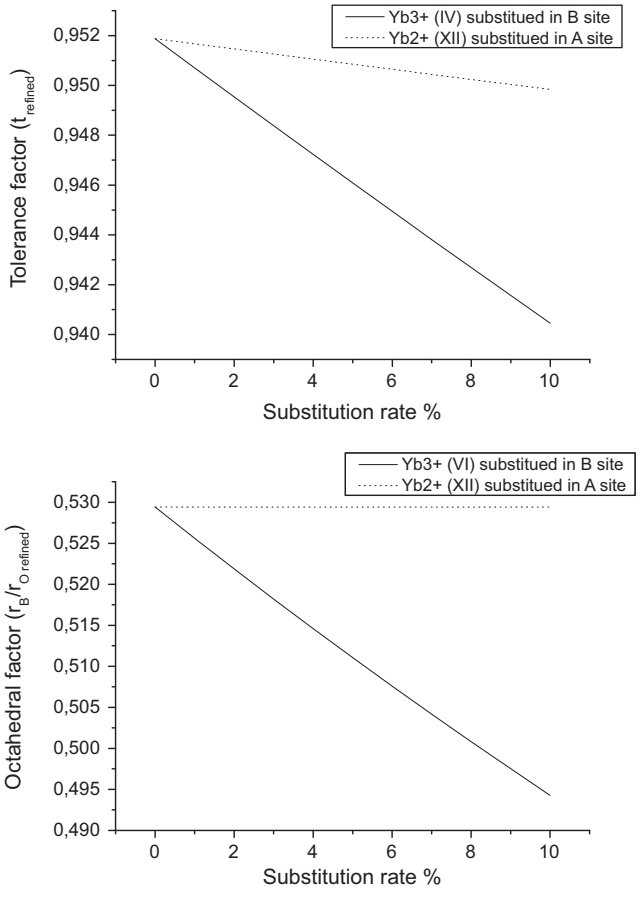

Fig. 11. $t_{refined}$ and $(r_B/r_O)_{refined}$ progression versus the substitution rate in A or B site of strontium zirconate.

4. Conclusions

This study shows the role of perovskite unit cell distortion on sintering rate. Increased distortion means increased densification. This distortion, measured by tolerance and refined octahedral factors, is due to the size of the cation radius A (Ba/Sr) and the lanthanide elements in substitution in the unit cell. Bivalent ions (Yb) can occupy A or B sites of the perovskite leading to the formation of alkaline earth oxide, of zirconia type phases and gaseous oxygen. These substitutions influence in different manners the sintering according to the distortion degree of the unit cell of the perovskite. Sintering atmospheres have no influence on the sintering rate of zirconia perovskite, which proves that anionic vacancies do not control the sintering.

Acknowledgements

The authors want to thank Christpoher Yukna and Jean-Baptiste Fruhauf for their help in proof reading and Huguette Bruyas for her help in XRD measurements.

References

[1] S. Imashuku, T. Uda, Y. Nose, Y. Awakura, J. Alloys Compd. 490 (2010) 672–676.
[2] C.-M. Fang, R. Ahuja, Phys. Earth Planet. Int. 157 (2006) 1–7.
[3] F. Iguchi, T. Tsurui, N. Sata, H. Yugami, Solid State Ionics 180 (2009) 563–568.
[4] H. Padma Kumar, C. Vijayakumar, C.N. George, S. Solomon, R. Jose, J.K. Thomas, J. Koshy, J. Alloys Compd. 458 (2008) 528–531.
[5] I. Antunes, G.C. Mather, J.R. Frade, J. Gracio, D.P. Fagg, J. Solids State Chem. 183 (2010) 2826–2834.
[6] A. Kumar, A.S. Verma, J. Alloys Compd. 480 (2009) 650–657.
[7] F. Giannici, A. Longo, K.D. Keurer, A. Balerna, A. Martorana, Solid State Ionics 181 (2010) 122–125.
[8] J.C. Sczancoski, L.S. Cavalcante, T. Badapanda, S.K. Rout, S. Panigrahi, V.R. Mastelaro, J.A. Varla, M. Siu Li, E. Longo, Solid State Sci. 12 (2010) 1160–1167.
[9] A. Sin, B. El Montaser, P. Odier, J. Am. Ceram. Soc. 85 (2002) 1928–1932.
[10] F.M.M. Snijkers, A. Buekenhoudt, J. Cooymans, J.J. Luyten, Scripta. Mater. 50 (3) (2004) 655–659.
[11] J.H. Tong, D. Clark, L. Bernau, M. Sanders, R. O'Hayre, J. Mater. Chem. 20 (2010) 6333–6341.
[12] D.Y. Gao, R.S. Guo, J. Alloys Compd. 493 (2010) 288–293.
[13] L.Q. Jiang, J.K. Guo, H.B. Liu, M. Zhu, X. Zhou, P. Wu, C.H. Li, J. Phys. Chem. Solids 67 (2006) 1531–1536.
[14] C. Li, K. Chi Kwan Soh, P. Wu, J. Alloys Compd. 372 (2004) 40–48.
[15] L. Liang, L. Wencong, C. Nianyi, J. Phys. Chem. Solids 65 (2004) 855–860.
[16] H. Ulmann, N. Trofimenko, J. Alloys Compd. 316 (2001) 153–158.
[17] V.N. Goldschmidt, Naturwissenschaften 14 (1926) 477.
[18] L.M. Feng, L.Q. Jiang, M. Zhu, H.B. Liu, X. Zhou, C.H. Li, J. Phys. Chem. Solids 69 (2008) 967–974.
[19] R.D. Shannon, Acta Crystallogr., Sect. A (1976) 751–767.
[20] N.E. Trofimenko, H. Ullman, J. Eur. Ceram. Soc. 20 (2000) 1241–1250.
[21] H. Ullman, N. Trofimenko, F. Tietz, D. Stver, A. Ahmad-Khanlou, Solid State Ionics 138 (2000) 79–90.